Journal of Dental Sciences 17 (2022) 1125–1134

Available online at www.sciencedirect.com

ScienceDirect

journal homepage: www.e-jds.com

Original Article

Circ_0138959/miR-495-3p/TRAF6 axis regulates proliferation, wound healing and osteoblastic differentiation of periodontal ligament cells in periodontitis

Wenjuan Deng [a], Xiaoliang Wang [a], Jin Zhang [a], Sainan Zhao [b*]

[a] *Department of Stomatology, Gaoxin Branch of Jinan Stomatological Hospital, Jinan, Shandong, China*
[b] *Department of Stomatology, Affiliated Hospital of Shandong University of Traditional Chinese Medicine, Jinan, China*

Received 6 December 2021; Final revision received 13 January 2022
Available online 15 February 2022

KEYWORDS
CircRNA;
miRNA;
TRAF6;
Periodontal ligament;
Periodontitis

Abstract *Background/purpose:* Periodontitis is a chronic inflammatory disease, and periodontal ligament cells (PDLCs) are pivotal for osteogenesis. Circular RNAs (circRNAs) can regulate disease progression via targeting miRNA/mRNA axis. The purposes of this study were to explore the function and mechanism of circ_0138959 in periodontitis.
Materials and methods: Periodontitis cell model was established by lipopolysaccharide (LPS) treatment in PDLCs. RNA expression was determined by quantitative reverse transcription-polymerase chain reaction assay. Cell proliferation was detected using 3-(4, 5-dimethylthiazol-2-y1)-2, 5-diphenyl tetrazolium bromide assay. Wound healing and cell apoptosis were examined by wound healing assay and flow cytometry. Inflammatory cytokines were measured via Enzyme-linked immunosorbent assay. Osteogenic differentiation was assessed by Alkaline phosphatase and Alizarin red S staining assays. Western blot was used for protein detection. The target interaction was validated by dual-luciferase reporter assay.
Results: Circ_0138959 was overexpressed in periodontitis tissues and LPS-treated PDLCs. Downregulation of circ_0138959 attenuated LPS-induced inhibition of proliferation, wound healing and osteogenic differentiation but promotion of apoptosis and inflammation. Circ_0138959 acted as a miR-495-3p sponge, and the regulatory role of circ_0138959 in LPS-induced cell injury was achieved by sponging miR-495-3p. Additionally, miR-495-3p targeted TNF Receptor Associated Factor 6 (TRAF6) and miR-495-3p protected against LPS-induced cell dysfunction by targeting TRAF6. Circ_0138959 upregulated TRAF6 level via inhibiting miR-495-3p.

* Corresponding author. Department of stomatology, Affiliated Hospital of Shandong University of Traditional Chinese Medicine, No. 16369, Jingshi Road, Jinan City, Shandong Province, 250014, China.
E-mail address: sainan82@163.com (S. Zhao).

https://doi.org/10.1016/j.jds.2022.01.010

Conclusion: This study suggested that circ_0138959 upregulated the TRAF6 expression by binding to miR-495-3p, consequently aggravating LPS-induced cell damages in PDLCs. Circ_0138959 might be a probable target for treatment of periodontitis.

Introduction

Periodontitis is an inflammatory disease characterized by the disruption of periodontal ligament.[1,2] Periodontitis patients have high risks to develop other systemic diseases.[3,4] A number of biological molecules have been found to regulate the progression of periodontitis.[5] Thus, discovering the molecular targets may contribute to the treatment of periodontitis. Periodontal ligament (PDL) is essential to maintain periodontal homeostasis and promote periodontal wound healing.[6] Periodontal ligament cells (PDLCs) are important cells isolated from PDL tissues.[7] Lipopolysaccharide (LPS) is a common risk factor to simulate the inflammatory environment of periodontitis *in vitro*. It is necessary to explore the functional roles of biomolecules in LPS-treated PDLCs.

Circular RNAs (circRNAs) are specific noncoding RNAs with important implications in various inflammatory diseases.[8] Wang et al. reported that circ-CDR1as mitigated LPS-induced inhibition of cell proliferation in periodontitis.[9] Zheng et al. found that circCDK8 inhibited osteogenic differentiation and induced cell apoptosis of PDLCs.[10] Li et al. discovered that circ_0062491 and circ_0095812 functioned as potential targets for periodontitis.[11] A recent circRNA expression profile indicated that circ_0138959 was significantly upregulated in periodontitis patients.[11] However, the regulatory role of circ_0138959 in periodontitis has not been researched.

CircRNAs can regulate disease progression by acting as microRNA (miRNA) sponges.[12] For example, circCDR1as and circ_0062491 affected the pathological development of periodontitis by sponging miR-7 and miR-584.[9,11] The expression of microRNA-495-3p (miR-495-3p) was downregulated in LPS-treated PDLCs.[13] Nevertheless, the function of miR-495-3p in periodontitis and the association with circ_0138959 are still unclear.

Small miRNAs also affect the pathogenesis of human diseases via targeting the 3′untranslated regions (3′UTRs) of downstream genes.[14] TNF Receptor Associated Factor 6 (TRAF6) induced the inflammatory response in LPS-induced periodontitis,[15] and miR-146a inhibited cell inflammation in periodontitis by targeting TRAF6.[16] In addition, circRNAs regulate gene expression levels through specific miRNA sponging function.[17] For instance, circ_0081572 suppressed the progression of periodontitis by sponging miR-378h to upregulate the level of RORA.[18] It is unknown whether circ_0138959 can regulate TRAF6 expression via targeting miR-495-3p.

The aims of this study were to explore the biological function and molecular mechanism of circ_0138959 in LPS-induced injury of PDLCs. Circ_0138959 was hypothesized as a sponge of miR-495-3p to regulate TRAF6 expression, intending to unravel a novel pathogenic mechanism underlying the progression of periodontitis.

Materials and methods

Sample collection

Periodontal ligament tissues were collected from the surface of the gingival sulcus of 35 chronic periodontitis (CP) patients during the premolar extraction at Gaoxin branch of Jinan stomatological hospital. The inclusion criteria of patients were as follows: (1) classification between moderate and severe CP; (2) at least one single-rooted tooth with clinical attachment loss (CAL) $>$ 4 mm, (3) probing depth (PD) $>$ 5 mm. The exclusion criteria of patients were listed as below: (1) patients with smoking; (2) patients with systemic diseases, such as rheumatoid arthritis and allergic type 1 or 2 diabetes; (3) patients with uptake antibiotics and corticosteroids within 1 month before the surgery. (4) patients with medical treatment. The demographic data of CP patients were gender (male/female): 22/13, age (years): 53 $\pm$ 9. Normal tissues were obtained 30 healthy individuals (male/female, 19:11; years, 55 $\pm$ 9). The inclusion criteria were CAL $<$4 mm, PD $<$ 4 mm, and no alveolar bone destruction at radiographic level. These samples were frozen in liquid nitrogen for further use. All subjects have signed the informed consent forms. The collection and use of samples were in accordance with the Helsinki Declaration. In addition, this study was authorized by the Ethics Committee of Gaoxin branch of Jinan stomatological hospital.

Cell culture and induction

PDLCs were isolated from periodontal ligaments of 26 teeth extracted for orthodontic treatment from 12 healthy individuals. Periodontal ligaments were carefully scraped off from the middle third of the roots and cut into 1 mm^3 pieces, then plated into the 35 mm cell culture dishes. The plates were cultured with Dulbecco's modified eagle medium (DMEM, Sigma, St. Louis, MO, USA) containing 10% fetal bovine serum and 1% antibiotics (100 U/mL penicillin and 100 μg/mL streptomycin; Gibco, Carlsbad, CA, USA) in 5% CO_2 incubator at 37 °C. The medium was changed every 7 days until the confluent cells were formed, then cells were passaged and the third-passage cells were used for further detection. To induce periodontitis-like injury,

PDLCs were treated with 1 μg/mL LPS (Sigma) for different times (12 h, 24 h, 48 h).

Cell transfection

After LPS treatment for 24 h, cell transfection was performed by Lipofectamine™ 3000 Kit (Invitrogen, Carlsbad, CA, USA). Briefly, 2×10^4 cells were plated into the 48-well plates and cultured to 70% confluence. Vectors or oligonucleotides were diluted with Opti-MEM® Reduced Serum Medium and mixed with Lipofectamine™ 3000 reagent, then cells were incubated with the complexes at 37 °C. The stable-transfected cell line was constructed by short hairpin RNA (shRNA) lentiviral vector (RIOBOBIO, Guangzhou, China) against circ_0138959 (sh-circ_0138959), with shRNA negative control (sh-NC) as the control group. The miR-495-3p mimic (miR-495-3p), miRNA NC mimic (miR-NC), miR-495-3p inhibitor (in-miR-495-3p) and miRNA NC inhibitor (in-miR-NC) were purchased from RIBOBIO. For overexpression of TRAF6, TRAF6 sequence was cloned into pcDNA expression plasmid (Invitrogen) to construct pcDNA-TRAF6 (TRAF6) plasmid.

The quantitative reverse transcription-polymerase chain reaction (qRT-PCR) assay

Total RNA was extracted by TRI Reagent (Sigma) and the complementary DNA (cDNA) was synthesized by ReverTra Ace® qPCR RT Kit (Toyobo, Kita-Ku, Osaka, Japan). Subsequently, 2 μg cDNA was used for PCR detection using SYBR® Green Realtime PCR Master Mix (Toyobo). Forward (F) and reverse (R) primers were bought from Sangon (Shanghai, China): circ_0138959: 5′-CGACTCTCCCATTGACCTGT-3' (F), 5′-CACCATTCTTTGGCCAGTTT-3' (R); guanine deaminase (GDA): 5′-CTGACATGTGTGCCGCTCAG-3' (F), 5′-CTATTTTGCC GCTGTCGCTC-3' (R); miR-495-3p: 5′-TCGGCAGGAAACAAA-CATGGTG-3' (F), 5′-CAACTGGTGTCGTGGAGT-3' (R); TRAF6: 5′-CAATGCCAGCGTCCCTTCCAAA-3' (F), 5′-CCAAAGGACAGTT CTGGTCATGG-3' (R); β-actin: 5′-CACCATTGGCAATGAGCGGT TC-3' (F), 5′-AGGTCTTTGCGGATGTCCACGT-3' (R); U6: 5′-CTCGCTTCGGCAGCACA-3' (F), 5′-AACGCTTCACGAATTTGCG T-3' (R). β-actin and U6 were used to standardize RNA expression levels, and data analysis was carried out using the $2^{-\Delta\Delta Ct}$ method.[19]

Stability assay

Total RNA was digested with 3 U/μg Ribonuclease R (RNase R; GENESEED, Guangzhou, China) at 37 °C for 1 h. Cells were exposed to 2 mg/mL Actinomycin D (Selleck, Houston, TX, USA) at 37 °C, then cells were collected at different times (0 h, 4 h, 8 h, 12 h, 24 h) and RNA was isolated from cells. Afterwards, circ_0138959 and linear GDA levels were quantified by qRT-PCR.

3-(4, 5-dimethylthiazol-2-y1)-2, 5-diphenyl tetrazolium bromide (MTT) assay

Cells were harvested after transfection for 0 h, 12 h, 24 h or 48 h. The proliferation ability was measured using MTT Cell Growth Kit (Sigma) following the manufacturer's guidance, then cell absorbance was analyzed at 570 nm under the microplate reader (Sigma).

Wound healing assay

Wound healing assay was used to determine cell migration. Two straight scratches were produced by a sterile pipette tip in monolayer PDLCs. Those waste cells were removed by phosphate buffer solution (PBS), then cells were maintained in serum-free DMEM medium at 37 °C for 24 h. The scratch width was measured at 0 h (A) and 24 h (B), and migration ratio was calculated as follows: $(A - B)/A \times 100\%$.

Flow cytometry

Cell apoptosis was examined using Annexin-FITC Apoptosis Staining Kit (Abcam, Cambridge, MA, USA). After cell culture for 72 h, 6×10^4 PDLCs were collected and resuspended in 1 × Binding Buffer. Then, cell suspension was incubated with 10 μL Annexin V-fluorescein isothiocyanate (FITC) and 5 μL propidium iodide (PI) in the dark for 20 min. The apoptotic cells (Annexin V+/PI- and Annexin V+/PI+) were distinguished through the fluorescence of Annexin-FITC (green) and PI (red) under the flow cytometer (BD Biosciences, San Diego, CA, USA). Cell apoptotic rate = apoptotic cells/total cells × 100%.

Enzyme-linked immunosorbent assay (ELISA)

1×10^4 PDLCs were cultured for 24 h in the 96-well plates, then cell supernatants were harvested after LPS treatment and different transfection. The concentrations of tumor necrosis factor-alpha (TNF-α) and interleukin-1β (IL-1β) were examined via Human TNF-α ELISA Kit and IL-1β ELISA Kit (Abcam), respectively. The detection of each sample was independently performed with three times (n = 3).

Alkaline phosphatase (ALP) and Alizarin red S (ARS) staining assays

Osteogenic differentiation was induced by supplementing with 100 nM dexamethasone, 200 μM L-ascorbic acid and 10 mM β-glycerophosphate (Sigma) into the growth medium. One week later, ALP staining was performed by BCIP/NBT Alkaline Phosphatase Color Development Kit (Beyotime, Shanghai, China) and ALP activity was analyzed by ALP activity colorimetric assay kit (BioVision, Milpitas, CA, USA). After incubation for two weeks, cells were dyed with 0.1% ARS (Sigma) and ARS quantification was examined as previously reported.[20] The images were saved at 100× magnification.

Western blot

The protein expression levels were determined according to the issued procedures.[21] Antibody information was exhibited as below: anti-ALP (Abcam, ab229126, 1:1000), anti-runt-related transcription factor 2 (anti-RUNX2;

Abcam, ab23981, 1:1000), anti-TRAF6 (Abcam, ab40675, 1:1000), anti-β-actin (Abcam, ab8227, 1:1000) and Goat Anti-rabbit IgG H&L (HRP) secondary antibody (Abcam, ab205718, 1:5000). The protein blots on the membranes were visualized by ECL Substrate Kit (Abcam), followed by protein expression analysis using ImageJ software (NIH, Bethesda, MD, USA).

Dual-luciferase reporter assay

The wild-type (WT) and mutant (MUT) plasmids were constructed for luciferase detection. Briefly, circ_0138959 or TRAF6 3′UTR sequence was cloned into pmirGLO plasmid (Promega, Madison, WI, USA) to generate the recombinant circ_0138959 WT and TRAF6 3′UTR WT plasmids (containing miR-495-3p binding sites). Additionally, circ_0138959 MUT and TRAF6 3′UTR MUT plasmids were obtained by inserting the mutated sequence (site mutation in miR-495-3p binding sites) into pmirGLO plasmid. PDLCs were co-transfected with circ_0138959 or TRAF6 plasmid and miR-NC or miR-495-3p for two days, followed by cell collection and luciferase activity detection using Dual-Luciferase Reporter Assay System (Promega).

Statistical analysis

The linear relationships between targets in tissue samples were analyzed by Pearson's correlation coefficient. Data were collected from three independent experiments and expressed as the mean ± standard deviation (SD). The statistical analysis was performed using SPSS 22.0 (SPSS Inc., Chicago, IL, USA). Group difference was assessed using Student's *t*-test and one-way analysis of variance (ANOVA) followed by Tukey's test. *P* value less than 0.05 indicated that statistical difference was significant.

Results

Circ_0138959 was highly expressed in periodontitis samples and LPS-treated PDLCs

Firstly, circ_0138959 expression was detected in the collected tissues from CP patients. The clinical characteristics were as follows: CP patients (PD: 5.73 ± 0.62 mm, CAL: 4.98 ± 0.55 mm, probe bleeding index: 3.37 ± 0.29) and healthy controls (PD: 2.04 ± 0.46 mm, CAL: 1.92 ± 0.38 mm). The qRT-PCR analysis demonstrated that circ_0138959 was significantly upregulated in tissue samples from CP patients compared with those samples from healthy controls (Fig. 1A). Also, circ_0138959 expression was higher in LPS treatment groups than that in control group (Fig. 1B). No significance of circ_0138959 level was observed between 24 h and 48 h, then 24 h LPS treatment was used in the subsequent research. Circ_0138959 expression was unaffected while linear GDA level was obviously downregulated after treatment of RNase R (Fig. 1C) and Actinomycin D (Fig. 1D), which suggested that circ_0138959 was highly stable. Therefore, circ_0138959

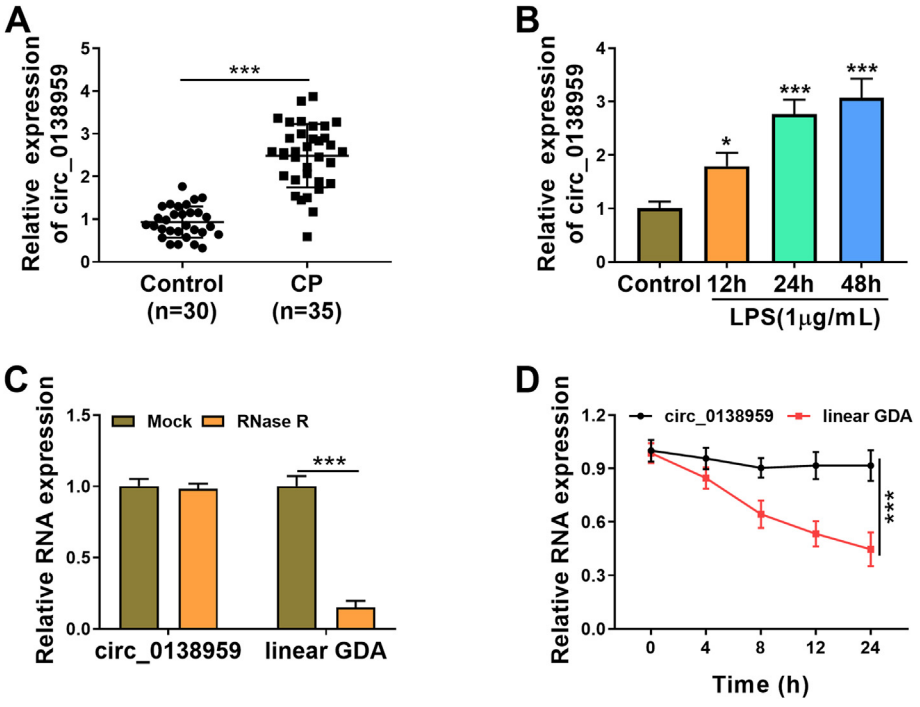

Figure 1 Circ_0138959 was highly expressed in periodontitis samples and LPS-treated PDLCs. (A—B) The expression of circ_0138959 was assayed via qRT-PCR in healthy and CP tissues (A), as well as LPS-treated PDLCs and control cells (B). (C—D) The stability of circ_0138959 was assessed via qRT-PCR after RNase R digestion in RNA (C) or Actinomycin D treatment in cells (D). $^{*}P < 0.05$, $^{***}P < 0.001$.

was an upregulated circRNA in periodontitis samples and LPS-treated PDLCs.

Silence of circ_0138959 facilitated proliferation, wound healing and osteogenic differentiation but repressed apoptosis and inflammation in LPS-treated PDLCs

Then, the role of circ_0138959 *in vitro* was investigated after knockdown of circ_0138959 expression. The qRT-PCR data affirmed that knockdown efficiency of sh-circ_0138959 was significant relative to sh-NC group (Fig. 2A). MTT and wound healing assays manifested that LPS treatment suppressed cell proliferation (Fig. 2B) and wound healing (Fig. 2C), whereas these influences were mitigated by transfection of sh-circ_0138959. Meanwhile, circ_0138959 expression inhibition abrogated LPS-induced enhancement of cell apoptosis (Fig. 2D) and release of TNF-α/IL-1β (Fig. 2E and F). ALP activity and ARS quantification were higher in LPS + sh-circ_0138959 group than LPS + sh-NC group, showing that circ_0138959 knockdown promoted osteogenic differentiation of LPS-treated PDLCs (Fig. 2G). In addition, Western blot results indicated that ALP and RUNX2 (osteogenic markers) protein levels were upregulated by sh-circ_0138959 in PDLCs with LPS treatment (Fig. 2H). Altogether, circ_0138959 downregulation reversed LPS-induced cell damages in PDLCs.

Circ_0138959 exerted the sponge-like effect on miR-495-3p

CircBank (http://www.circbank.cn/index.html) was used for bioinformatics analysis between circ_0138959 and miR-495-3p. The binding sites of miR-495-3p were

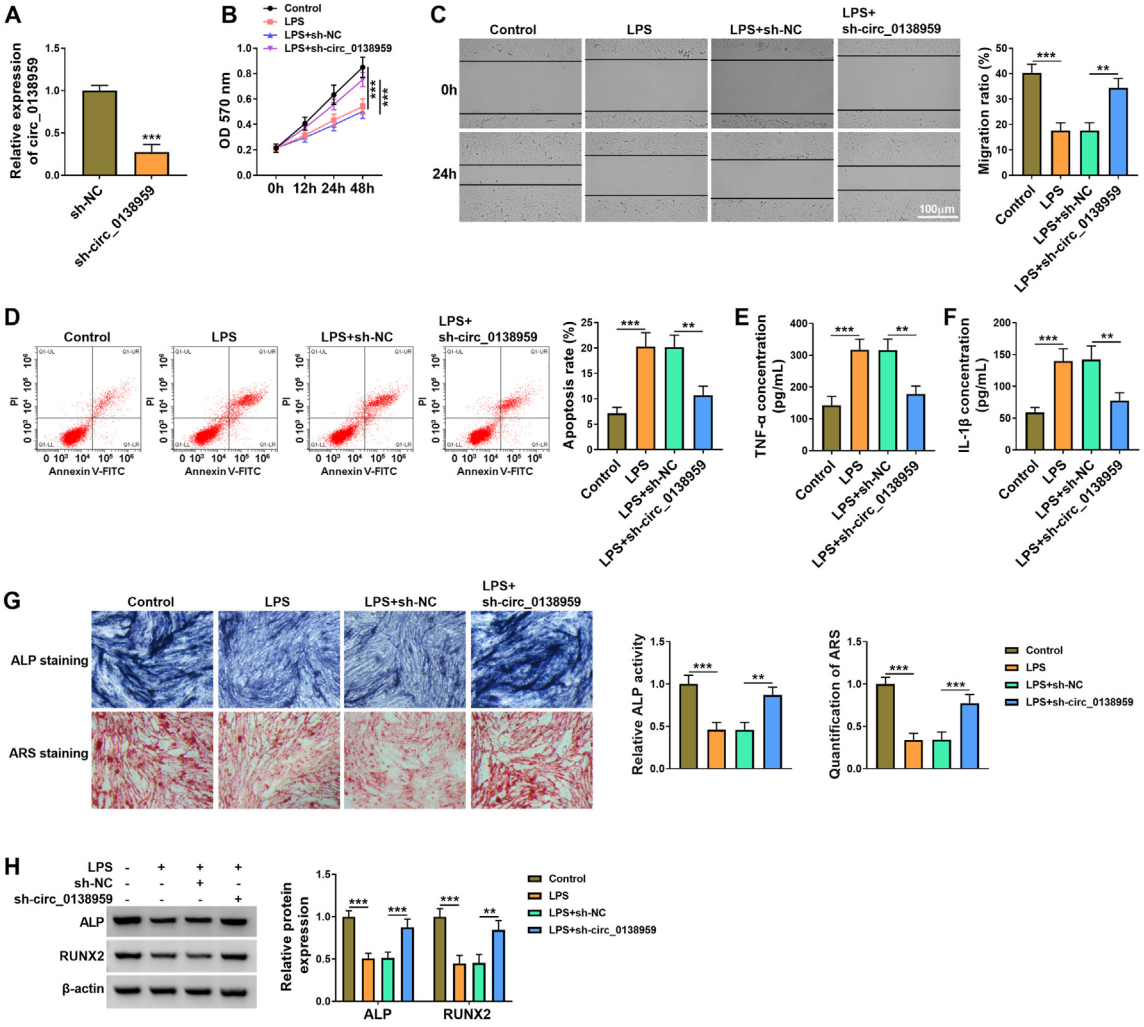

Figure 2 Silence of circ_0138959 facilitated proliferation, wound healing and osteogenic differentiation but repressed apoptosis and inflammation in LPS-treated PDLCs. (A) The circ_0138959 level was determined using qRT-PCR in sh-NC or sh-circ_0138959-transfected PDLCs. (B–H) PDLCs were treated with control, LPS, LPS + sh-NC or LPS + sh-circ_0138959. (B–C) Cell proliferation (B) and migration (C) were respectively measured using MTT assay and wound healing assay. (D–F) Cell apoptosis (D) and inflammation (E–F) were respectively evaluated using flow cytometry and ELISA. (G) Osteogenic differentiation was assessed by ALP activity and ARS quantification via the detection kits. (H) The protein levels of ALP and RUNX2 were examined using Western blot. $^{**}P < 0.01$, $^{***}P < 0.001$.

predicted in circ_0138959 sequence (Fig. 3A). The miR-495-3p mimic was used for overexpression of miR-495-3p, and qRT-PCR analysis showed that transfection efficacy was great in PDLCs (Fig. 3B). The interaction between circ_0138959 and miR-495-3p was confirmed by dual-luciferase reporter assay. As exhibited in Fig. 3C, luciferase activity was reduced after co-transfection with circ_0138959-WT and miR-495-3p but not circ_0138959-MUT and miR-495-3p. LPS treatment downregulated miR-495-3p expression in PDLCs compared to control group (Fig. 3D). Interestingly, miR-495-3p level was upregulated after knockdown of circ_0138959 in PDLCs (Fig. 3E). Also, miR-495-3p downregulation was detected in CP patients contrasted with healthy controls (Fig. 3F). There was a negative relation ($r = -0.6673$, $P < 0.001$) between expression levels of miR-495-3p and circ_0138959 in periodontitis samples (Fig. 3G). Hence, circ_0138959 could target miR-495-3p to act as a miRNA sponge.

Circ_0138959/miR-495-3p axis regulated the LPS-induced cell injury in PDLCs

To explore the association between miR-495-3p and circ_0138959 in periodontitis, the reverted experiments were performed in LPS-treated PDLCs. The miR-495-3p level was reduced by approximately 70% after in-miR-495-3p transfection in PDLCs, compared to in-miR-NC group (Fig. 4A). The effects of sh-circ_0138959 on cell proliferation (Fig. 4B), wound healing (Fig. 4C), apoptosis (Fig. 4D) and inflammatory response (Fig. 4E and F) in LPS-treated PDLCs were all attenuated by miR-495-3p inhibitor. ALP/ARS staining (Fig. 4G) and ALP/RUNX2 protein detection (Fig. 4H) revealed that miR-495-3p downregulation alleviated sh-circ_0138959-induced osteogenic differentiation. These data suggested that the function of circ_0138959 in periodontitis was partly related to the sponge effect on miR-495-3p.

TRAF6 was a downstream target of miR-495-3p

Through the online prediction by starbase (http://starbase.sysu.edu.cn), TRAF6 3′UTR sequence was shown to contain the binding sites for miR-495-3p (Fig. 5A). Furthermore, upregulation of miR-495-3p reduced the luciferase activity of TRAF6 3′UTR-WT plasmid while no significant change was found in TRAF6 3′UTR-MUT plasmid (Fig. 5B). The expression analysis exhibited that TRAF6 mRNA and protein levels were upregulated in LPS-treated PDLCs relative to control group (Fig. 5C and D). The qRT-PCR and Western blot assays displayed that overexpression of miR-495-3p induced mRNA and protein expression inhibition of TRAF6, but miR-495-3p inhibitor triggered opposite effects (Fig. 5E and F). Thus, miR-495-3p targeted TRAF6 to induce the direct expression change.

Circ_0138959 functioned as a miR-495-3p sponge to regulate TRAF6 expression

Moreover, TRAF6 protein expression was downregulated by sh-circ_0138959 and this regulation was counteracted after

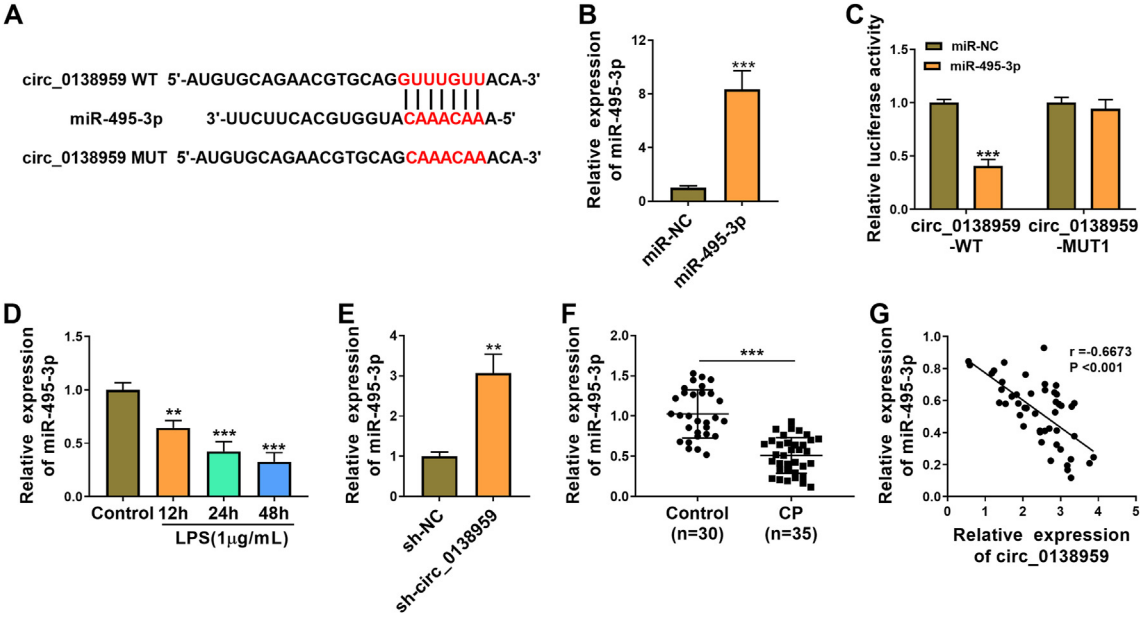

Figure 3 Circ_0138959 exerted the sponge-like effect on miR-495-3p. (A) The binding sites between circ_0138959 and miR-495-3p were shown by circBank. (B) The level of miR-495-3p was quantified using qRT-PCR in PDLCs transfected with miR-NC or miR-495-3p. (C) Dual-luciferase reporter assay was applied to analyze the interaction between circ_0138959 and miR-495-3p in PDLCs. (D) The qRT-PCR was performed for the detection of miR-495-3p in LPS-treated PDLCs. (E) The miR-495-3p expression was measured by qRT-PCR after transfection of sh-NC and sh-circ_0138959. (F) The miR-495-3p quantification was conducted by qRT-PCR in CP and control samples. (G) Pearson's correlation coefficient was used for analyzing the relationship between circ_0138959 and miR-495-3p in CP tissues. $^{**}P < 0.01$, $^{***}P < 0.001$.

miR-495-3p inhibition (Fig. 6A). The mRNA and protein levels of TRAF6 were upregulated in CP tissues compared with control tissues (Fig. 6B and C). Pearson's correlation coefficient showed that TRAF6 mRNA level was negatively associated with miR-495-3p expression ($r = -0.6511$, $P < 0.001$) (Fig. 6D), but it was positively related to circ_0138959 level ($r = 0.6068$, $P < 0.001$) (Fig. 6E) in CP samples. TRAF6 was regulated by circ_0138959 via targeting miR-495-3p. In addition, TRAF6 overexpression has relieved the protective effects of miR-495-3p for LPS-treated PDLCs (Supplementary Fig. 1). Taken together, circ_0138959 regulated LPS-induced injury by affecting miR-495-3p-mediated TRAF6 expression.

Discussion

CircRNAs are a crucial class of functional regulators in a variety of diseases. This study provided evidences to clarify that circ_0138959 contributed to the progression of periodontitis by targeting miR-495-3p/TRAF6 axis *in vitro*.

The quantification detection exhibited that circ_0138959 was highly expressed in periodontitis tissues, which was in accordance with the previous research.[11] Meanwhile, circ_0138959 was found to be upregulated in LPS-treated PDLCs. CircRNA dysregulation is correlated to various kinds of biological processes in human diseases. Zeng et al. stated that circRNF180 upregulation reduced cell proliferation,

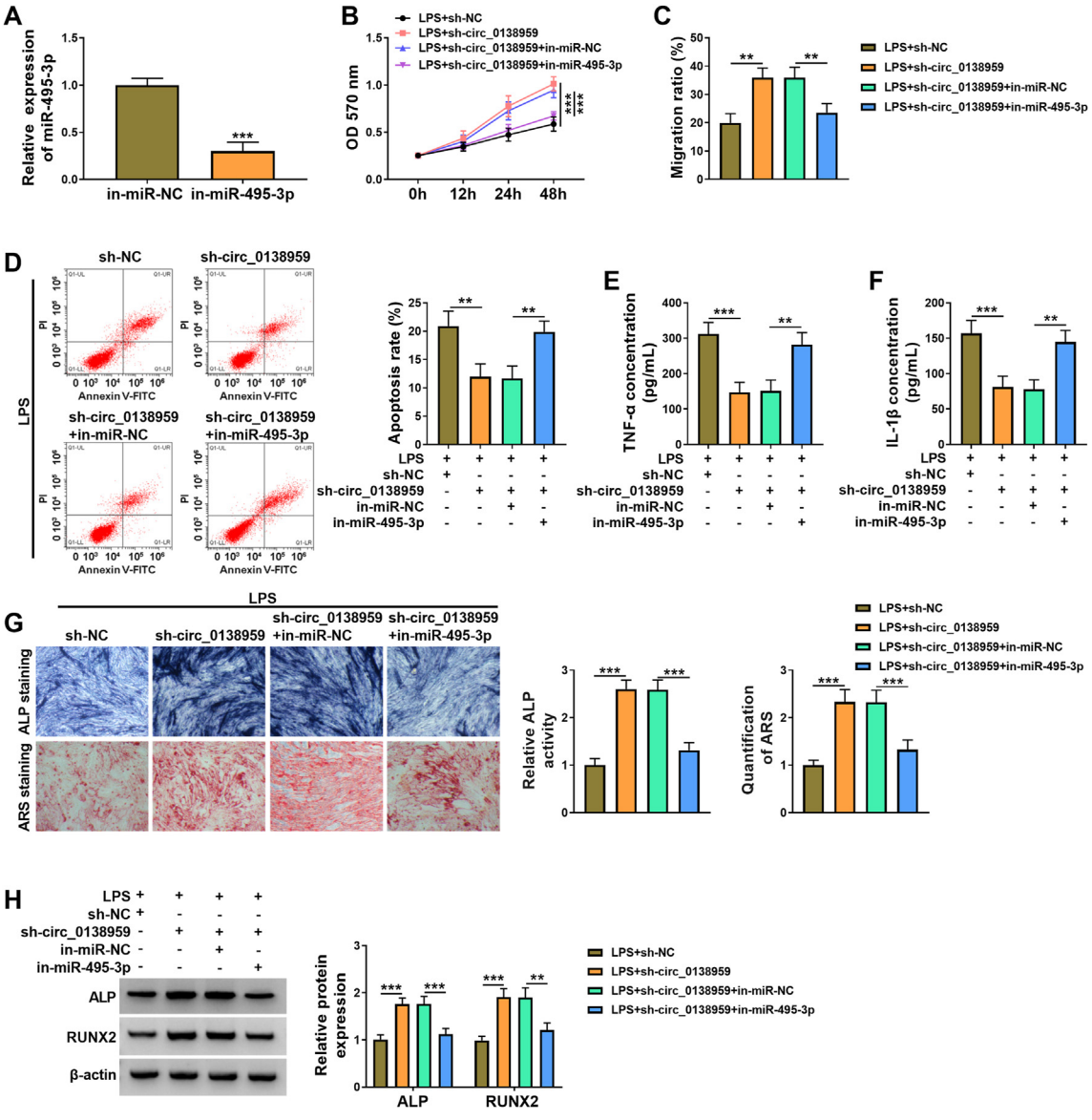

Figure 4 Circ_0138959/miR-495-3p axis regulated the LPS-induced cell injury in PDLCs. (A) The miR-495-3p expression analysis was carried out by qRT-PCR after transfection of in-miR-NC or in-miR-495-3p. (B–H) PDLCs were treated with LPS + sh-NC, LPS + sh-circ_0138959, LPS + sh-circ_0138959+in-miR-NC or LPS + sh-circ_0138959+in-miR-495-3p. (B–C) MTT and wound healing assays were performed to examine cell proliferation (B) and migration (C), respectively. (D–F) Flow cytometry and ELISA were conducted to determine cell apoptosis (D) and inflammatory cytokines (E–F), respectively. (G–H) ALP activity/ARS quantification assays (G) and ALP/RUNX2 protein levels (H) were used to assess osteogenic differentiation. $^{**}P < 0.01$, $^{***}P < 0.001$.

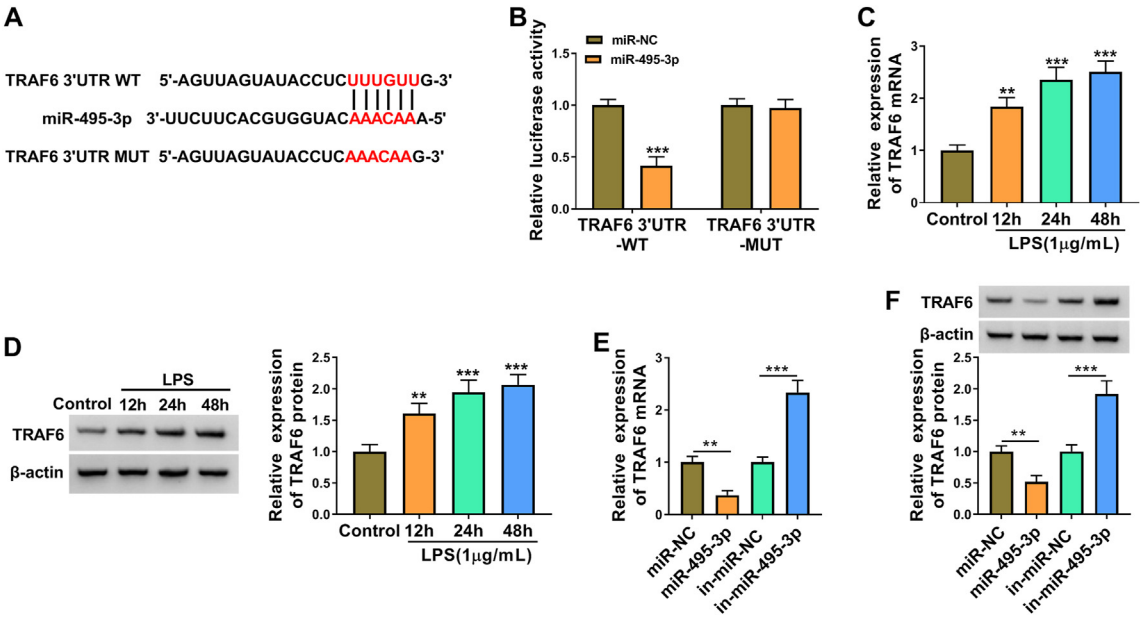

Figure 5 TRAF6 was a downstream target of miR-495-3p. (A) Starbase exhibited the potential binding between TRAF6 and miR-495-3p. (B) The interaction between TRAF6 and miR-495-3p was affirmed via dual-luciferase reporter assay. (C—D) The qRT-PCR and Western blot were performed for expression detection of TRAF6 in LPS-treated PDLCs. (E—F) TRAF6 mRNA and protein levels were examined using qRT-PCR and Western blot after transfection of miR-495-3p, in-miR-495-3p or the relative control groups. $^{**}P < 0.01$, $^{***}P < 0.001$.

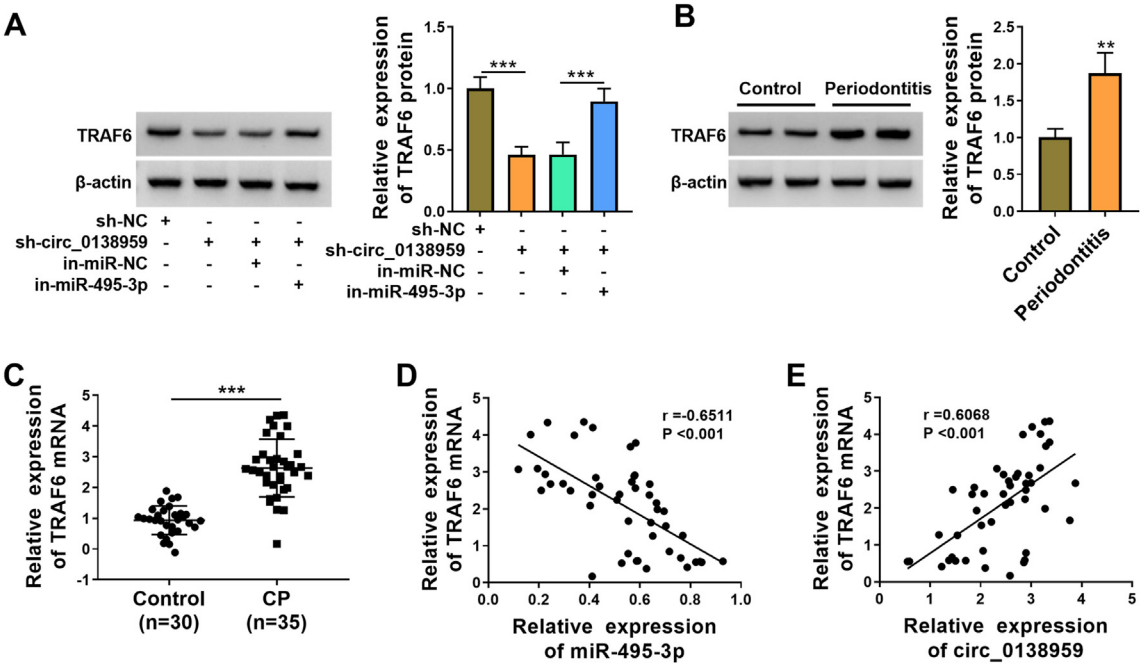

Figure 6 Circ_0138959 functioned as a miR-495-3p sponge to regulate TRAF6 expression. (A) TRAF6 protein expression was analyzed via Western blot after PDLCs were transfected with sh-NC, sh-circ_0138959, sh-circ_0138959+in-miR-NC or sh-circ_0138959+in-miR-495-3p. (B—C) The protein (B) and mRNA (C) detection for TRAF6 was conducted using Western blot and qRT-PCR in CP and control tissues. (D—E) The linear relation between TRAF6 and miR-495-3p (D) or circ_0138959 (E) was analyzed by Pearson's correlation coefficient. $^{**}P < 0.01$, $^{***}P < 0.001$.

invasion and migration in hepatocellular carcinoma.[22] Knockdown of circ_0134111 suppressed cell apoptosis and inflammation reaction in osteoarthritis.[23] High level of circRNA_103516 was used for clinical diagnosis of inflammatory bowel disease.[24] Our data demonstrated that circ_0138959 downregulation alleviated LPS-caused

inhibition of cell proliferation and wound healing, as well as acceleration of cell apoptosis and inflammatory response. Additionally, circ_0138959 knockdown contributed to osteogenic differentiation in LPS-treated PDLCs. Thus, circ_0138959 facilitated the progression of periodontitis *in vitro*. Circ_0138959 might be a diagnostic biomarker for periodontitis, and circ_0138959 expression inhibition could be used for the clinical treatment.

Furthermore, we validated the target interaction between circ_0138959 and miR-495-3p. The biological regulation of circRNA was closely related to miRNA sponging function. Circ_Lrp6 served as a natural miR-145 sponge to regulate vascular smooth muscle cell activity in atherosclerosis,[25] and circKMT2E promoted the progression of diabetic cataract by sponging miR-204-5p.[26] The current data indicated that circ_0138959 was involved in LPS-induced periodontitis progression via absorbing miR-495-3p.

Xu et al. reported that TRAF6 acted as a target for miR-495-3p in septic acute kidney injury.[27] Consistently, our target analysis exhibited that miR-495-3p directly targeted TRAF6. Moreover, circ_0138959 upregulated TRAF6 expression via targeting miR-495-3p. CircRNA/miRNA/mRNA axis has been disclosed as an important mechanism in human diseases. For example, circ_0074027 accelerated the malignant development of non-small cell lung cancer by upregulating Ras homolog gene family member A (RHOA) via binding to miR-2467-3p.[28] CircRNA_000203 has participated in the pathogenesis of cardiac hypertrophy via inhibiting the interaction between miR-140-3p or miR-26b-5p and Gata-binding protein 4 (Gata4).[29] Circ_0081572 inhibited the progression of periodontitis via targeting miR-378h to regulate the level of retinoid acid-related orphan receptor A (RORA).[18] Herein, miR-495-3p was shown to protect against LPS-induced cell damages in PDLCs by targeting TRAF6. These collective results elucidated that circ_0138959 promoted periodontitis progression via mediating miR-495-3p/TRAF6 axis.

However, this study still has some limitations. Firstly, data were acquired from cell experiments *in vitro*. More evidences in clinical patients may provide support for the current conclusion. Secondly, only miR-495-3p/TRAF6 axis was validated to be responsible for circ_0138959 function. It will be interesting to explore whether other miRNA/mRNA axes are associated with circ_0138959 in periodontitis. Thirdly, exploring the downstream signaling pathways of circ_0138959/miR-495-3p/TRAF6 may contribute to understanding the molecular mechanism of periodontitis. At last but not the least, precursor miRNAs with biological function can be detected using miRNA primers. It should be noted in future study.

In conclusion, this study indicated that circ_0138959 accelerated the pathological progression of periodontitis *in vitro* by regulating miR-495-3p/TRAF6 axis. More importantly, the treatment for periodontitis might be improved through reducing the expression of circ_0138959.

Declaration of competing interest

The authors have no conflicts of interest relevant to this article.

Acknowledgements

This work was supported by Shandong Provincial Nature Science Foundation (ZR2020QH334).

Appendix A. Supplementary data

Supplementary data to this article can be found online at https://doi.org/10.1016/j.jds.2022.01.010.

References

1. Sczepanik FSC, Grossi ML, Casati M, et al. Periodontitis is an inflammatory disease of oxidative stress: we should treat it that way. *Periodontol 2000* 2020;84:45—68.
2. Tsukasaki M. RANKL and osteoimmunology in periodontitis. *J Bone Miner Metabol* 2021;39:82—90.
3. Preshaw PM, Bissett SM. Periodontitis and diabetes. *Br Dent J* 2019;227:577—84.
4. Mesa F, Magan-Fernandez A, Castellino G, et al. Periodontitis and mechanisms of cardiometabolic risk: novel insights and future perspectives. *Biochim Biophys Acta (BBA) - Mol Basis Dis* 2019;1865:476—84.
5. Schaefer AS. Genetics of periodontitis: discovery, biology, and clinical impact. *Periodontol 2000* 2018;78:162—73.
6. Komaki M. Pericytes in the periodontal ligament. *Adv Exp Med Biol* 2019;1122:169—86.
7. Kim BC, Bae H, Kwon IK, et al. Osteoblastic/cementoblastic and neural differentiation of dental stem cells and their applications to tissue engineering and regenerative medicine. *Tissue Eng Part B Rev* 2012;18:235—44.
8. Marques-Rocha JL, Samblas M, Milagro FI, et al. Noncoding RNAs, cytokines, and inflammation-related diseases. *Faseb J* 2015;29:3595—611.
9. Wang F, Chen X, Han Y, Xi S, Wu G. circRNA CDR1as regulated the proliferation of human periodontal ligament stem cells under a lipopolysaccharide-induced inflammatory condition. *Mediat Inflamm* 2019;2019:1625381.
10. Zheng J, Zhu X, He Y, et al. CircCDK8 regulates osteogenic differentiation and apoptosis of PDLSCs by inducing ER stress/autophagy during hypoxia. *Ann N Y Acad Sci* 2021;1485:56—70.
11. Li J, Xie R. Circular RNA expression profile in gingival tissues identifies circ_0062491 and circ_0095812 as potential treatment targets. *J Cell Biochem* 2019;120:14867—74.
12. Lou Z, Zhou R, Su Y, et al. Minor and major circRNAs in virus and host genomes. *J Microbiol* 2021;59:324—31.
13. Du A, Zhao S, Wan L, et al. MicroRNA expression profile of human periodontal ligament cells under the influence of Porphyromonas gingivalis LPS. *J Cell Mol Med* 2016;20:1329—38.
14. Afonso-Grunz F, Muller S. Principles of miRNA-mRNA interactions: beyond sequence complementarity. *Cell Mol Life Sci* 2015;72:3127—41.
15. Tang L, Zhou XD, Wang Q, et al. TNF receptor-associated factor 6 suppression inhibits inflammatory response to Porphyromonas gingivalis in human periodontal ligament cells. *Quintessence Int* 2011;42:787—96.
16. Tang L, Li X, Bai Y, Wang P, Zhao Y. MicroRNA-146a negatively regulates the inflammatory response to Porphyromonas gingivalis in human periodontal ligament fibroblasts via TRAF6/p38 pathway. *J Periodontol* 2019;90:391—9.
17. Zhang L, Zhang Y, Wang Y, et al. Circular RNAs: functions and clinical significance in cardiovascular disease. *Front Cell Dev Biol* 2020;8:584051.

18. Wang J, Du C, Xu L. Circ_0081572 inhibits the progression of periodontitis through regulating the miR-378h/RORA axis. *Arch Oral Biol* 2021;124:105053.
19. Livak KJ, Schmittgen TD. Analysis of relative gene expression data using real time quantitative PCR and the 2(-Delta Delta C(T)) method. *Methods* 2001;25:402—8.
20. Li X, Zheng Y, Zheng Y, et al. Circular RNA CDR1as regulates osteoblastic differentiation of periodontal ligament stem cells via the miR-7/GDF5/SMAD and p38 MAPK signaling pathway. *Stem Cell Res Ther* 2018;9:232.
21. Kong L, Sun M, Jiang Z, Li L, Lu B. MicroRNA-194 inhibits lipopolysaccharide-induced inflammatory response in nucleus pulposus cells of the intervertebral disc by targeting TNF receptor-associated factor 6 (TRAF6). *Med Sci Mon Int Med J Exp Clin Res* 2018;24:3056—67.
22. Zeng X, Tan C, Mo M, et al. CircRNA profiling identifies circRNF180 as a tumor suppressor in hepatocellular carcinoma. *Epigenomics* 2021;13:513—30.
23. Wu R, Zhang F, Cai Y, et al. Circ_0134111 knockdown relieves IL-1beta-induced apoptosis, inflammation and extracellular matrix degradation in human chondrocytes through the circ_0134111-miR-515-5p-SOCS1 network. *Int Immunopharm* 2021;95:107495.
24. Ye YL, Yin J, Hu T, et al. Increased circulating circular RNA_103516 is a novel biomarker for inflammatory bowel disease in adult patients. *World J Gastroenterol* 2019;25:6273—88.
25. Hall IF, Climent M, Quintavalle M, et al. Circ_Lrp6, a Circular RNA Enriched in vascular smooth muscle cells, acts as a sponge regulating miRNA-145 function. *Circ Res* 2019;124:498—510.
26. Fan C, Liu X, Li W, et al. Circular RNA circ KMT2E is up-regulated in diabetic cataract lenses and is associated with miR-204-5p sponge function. *Gene* 2019;710:170—7.
27. Xu L, Cao H, Xu P, Nie M, Zhao C. Circ_0114427 promotes LPS-induced septic acute kidney injury by modulating miR-495-3p/TRAF6 through the NF-kappaB pathway. *Autoimmunity* 2021;55:52—64.
28. Duan Z, Wei S, Liu Y. Circ_0074027 contributes to non-small cell lung cancer progression through positively modulating RHOA via sequestering miR-2467-3p. *J Bioenerg Biomembr* 2021;53:223—33.
29. Li H, Xu JD, Fang XH, et al. Circular RNA circRNA_000203 aggravates cardiac hypertrophy via suppressing miR-26b-5p and miR-140-3p binding to Gata4. *Cardiovasc Res* 2020;116:1323—34.